https://doi.org/10.33472/AFJBS.6.2.2024.612-633

African Journal of Biological Sciences

Research Paper Open Access

Potential mitigating effect of Arabic Gum on Zink oxide induced cardiotoxicity in adult male albino rats

Nehal A. Amer [a], Noha M. Halloull [b*], Eman Mahmoud FaragAllah [c], Noura M. S. Osman [d] and Nehal E. Refaay [a]

[a] Human Anatomy & Embryology Department, Faculty of Medicine, Zagazig University, Egypt.

[b] Forensic medicine & Clinical toxicology Department, Faculty of Medicine, Zagazig University, Egypt.

[c] Physiology Department, Faculty of Medicine, Zagazig University, Egypt.

[d] Anatomy Department, Faculty of medicine. Port Said University. Egypt

***Corresponding author**: Noha M. Halloull

Forensic medicine & Clinical toxicology Department, Faculty of Medicine, Zagazig University, Egypt.

Tel: 00201095889478

Email: Nohahalol1981@gmail.com

Article History

Volume 6, Issue 2, April 2024

Received:19 April 2024

Accepted: 10 May 2024

Published: 16 May 2024

doi: 10.33472/AFJBS.6.2.2024.612-633

Abstract: Zinc Oxide nanoparticles (ZnO-NPs) are widely used in pharmaceuticals, foods, cosmetics, and toothpaste. The cardiovascular system is one of the most vulnerable exposed tissues to ZnO-NPs. Arabic Gum (AG) is an antioxidant that can be utilized to treat tissue injury. The purpose of this study was to investigate ZnO-NPs-induced cardiotoxicity and the potential protective role of AG. The study included 60 adult male albino rats. They were separated into 3 main groups of 20 rats each (control, ZnO-NPs treated, and protected AG+ ZnO-NPs). Each main group is equally subdivided into 2 subgroups with 10 rats each (control negative with no treatment at all, control positive received AG), ZnO-NPs (100 mg/kg Body weight(BW) and 400mg/kg/BW) and protected (AG + 100 mg/kg ZnO-NPs, AG+ 400 mg/kg ZnO-NPs). The dose of AG was 15 mg/kg/BW for tested groups receiving it as was mentioned. The medications were administered orally once a day for four weeks. When comparing the ZnO-NPs treated group versus the control one, there was a substantial rise in mean values of heart enzymes and inflammatory cytokines. Also cardiac histological analysis revealed deteriorated myocardium, vacuolated cytoplasm, and increased fibrosis with apoptosis in ZnO-NPs treated rats. These results were improved by concomitant administration of AG..

Keywords: Zink oxide nanoparticles, cardiotoxicity, heart enzymes, cytokines, fibrosis and Arabic Gum.

Introduction: Nanoparticles may be natural or synthetic, Metal nanoparticles (such as gold and silver nanoparticles), and metal oxide nanoparticles (such as zinc oxide) are some of the different forms of artificial nanoparticles. Artificial nanoparticles have different

physicochemical properties and reactivity from bigger equivalents of the same substance due to both tiny size and enormous surface area (Kao et al., 2012).

In recent decades, nanotechnology has become a potential method for variable biomedical applications. Among the most popular nanomaterials in industrial and domestic settings is zinc oxide nanoparticles (ZnO-NPs). (ZnO-NPs) were used as therapeutic agents, aesthetics, dietary supplements, apparel, sunscreens, sporting activities agents, and also in many consumer goods (Liu et al., 2016).

The Food and Drug Administration (FDA) has licensed zinc oxide nanoparticles as a novel and effective cancer therapeutics (Vinardell and Mitjans, 2015). By creating an imbalance in zinc-dependent enzyme production and producing oxygen-free radicals, zinc oxide nanoparticles can cause anticancer potential against tumor cells (Rasmussen et al., 2010). Research published in recent years have reported the use of zinc oxide nanoparticles as both medicinal agents and gene carriers. Several published studies also demonstrated the toxicity of zinc oxide nanoparticles on a variety of tissues and cell types. Particle high solubility was thought to cause hazardous impacts such as cytotoxic effects, peroxidation, and mitochondrial dysfunction (Condello et al., 2016).

Because of its tiny size, ZnO-NPs are able to penetrate human tissue by different ways: with food preparation, inhalation, and skin contact. ZnO-NPs diffuse into numerous tissues and organs via systemic circulation, including the liver, pancreas, renal tissue, and heart (Li et al., 2012). The Previous authors discovered that the introduction of zinc oxide nanoparticles by mouth or intraperitoneally caused the molecules to accumulate dangerously in the lung, spleen, hepatic and renal tissues as well as to spread throughout the body. Additionally, it was shown that administering zinc oxide nanoparticles to rodents' hepatocytes and hearts caused serious anemia and notable histological alterations. Pathological abnormalities included hyaline degeneration of the heart muscle as well as localized hemorrhages consistent with hepatic apoptosis (Esmaeillou et al., 2013).

Arabic Gum (AG) is a natural dry exudate produced by Acacia trees, specifically Acacia Senegal and Acacia seyal (Ali et al., 2009). It is frequently linked to health improvement by lowering the chances of developing metabolic syndrome (Met S). The health effects of AG are believed to be caused by 3 different components of high-branched sugar molecules which differ in their weight and protein constituents. These are typically referred to as arabinogalactan-protein fractions, arabinogalactan, and glycoprotein fractions (Williams and Phillips, 2021). On the other hand, the source, the climatic condition, and the soil can all affect AG structure (Jarrar et al., 2021). In 1969, the US Food and Drug Administration (FDA) authorized AG as a food additive. Following that time, it has a widespread application in the food industries as a preservative and emollient (Mahdavi et al., 2016). Additionally, it is utilized as a supplement to improve the physical effects of medications as well as constituent of sticky hydrogels for the treatment of wounds (Sun et al., 2016). Additionally, AG has antioxidant and anti-inflammatory effects, which means it could be utilized to treat

inflammation. It also appears to slow the course of chronic renal failure (Al Za'abi et al., 2018)

As a result, the purpose of the current investigation is to evaluate if ingesting AG could lessen the adverse impacts of ZnO-NPs upon the cardiac tissue. This investigation into such interaction is the first.

Materials and Methods:

Chemicals

Zink oxide nanoparticles: The average component dimension of zinc oxide nanoparticles had been beneath 35 nm, and their dispersion comprised under 100 nm. The lot/number MKBN3534V-Nano - SunguardTM in water had a concentration of 50% in H_2O and a water-based pH of 7 ± 0.1. Sigma-Aldrich Co., St. Louis, USA, produced the zinc oxide nanoparticles (Kim et al., 2012). Instantly prior to administration, distilled water was used to dissolve ZnO-NPs.

Gum Arabic was purchased from the local market, Cairo, Egypt; as spherical tears which were grinded to create a purified powdered form. 100 cc of warm water was used to dissolve 10 grams of the powder.

Animals

Throughout this study, 60 healthy adult male Sprague Dawley albinos have been collected from the animal house of the Faculty of Medicine at Zagazig University. Their weights ranged from 200 to 250 g. Those animals were housed in hygienic circumstances using ventilated polypropylene boxes with stainless steel covers and bedding made of wood shavings, supplied on a regular basis, and allowed access to running water. Their temperature was kept at 23±2 degrees Celsius. Rats spent two weeks getting used to the lab setting before this study started. The experiment's rats were handled in compliance with Zagazig University Institutional Animal Care and Use Committee (ZU-IACUC committee) and approval number (ZU-IACUC/3/F/246/2023*)*. The experiment was carried out according to ARRIVE guidelines.

Experimental protocol

Rats were grouped among three primary groups at random, and for 28 days, the rats received their medication by oral ingestion.

1- Group 1: Control group (20 rats); that was divided equally into 2 subgroups (10 rats each) :(negative control(NC) subgroup with no treatment all through the experiment, positive control(PC) subgroup in which rats were treated with AG. The dose of AG was 15 mg/kg/ B.W./day according to (Al-Doaiss and Al-Shehri, 2020).
2- Group 2: ZnO-NPs treated group (20 rats); that was divided into 2 equal subgroups (10 rats each) low dose subgroup in which rats received 100 mg ZnO-NPs /kg body weight and high dose subgroup in which rats were treated with 400mg ZnO-NPs /kg body weight (Pasupuleti et al., 2012).

3- Group 3: AG/ ZnO-NPs group (20 rats) ,that was divided into 2 equal subgroups (10 rats each) (AG/100 ZnO-NPs group, and AG/ ZnO-NPs 400 group). The dose of AG was 15 mg/kg/ B.W./day according to (Al-Doaiss and Al-Shehri, 2020).

Sample preparation

12 hours after finishing the latest treatment, total body rats' weights were reported before being given 50 mg/i.p. sodium phenobarbital as anesthesia. Within two minutes, the Bio-Amp acquired ECG characteristics, including heart rate (beats per minute), R-R interval (seconds), QRS interval (seconds), QT interval (seconds), QTc (seconds), QRS (mV), and T amplitude (mV). The Power Lab system subsequently tracked the collected data (AD-Instruments, Australia). Then with a sterile syringe, blood was drawn throughout the heart puncture. For hematological measures, Blood specimens were placed in EDTA-filled weatherman syringes. After centrifuging the non-heparinized blood for 10 min at 4000 rpm to ascertain its biochemical properties, the sera were collected and kept. Each chest cavity of different members of different studied groups was opened, the heart was removed, and each heart weight was recorded.

Homogenate tissue analysis for cardiac enzymatic activities

Lactate dehydrogenase (LDH; E.C.1.1.1.27) was measured using Deutsche technique (Bénéteau-Burnat and Baudin, 1991). The International Federation for Clinical Chemistry's method was used to measure the level of Creatine kinase (CK-MB) (EC: 2.7.3.2) in the heart (Bakhet, 2007). Cardiac Troponin-T (cTnT) as it is discharged into the bloodstream, cTnT is commonly utilized as a diagnostic biomarker for myocardial cellular damage owing to its higher cardio-specificity. The Biochemistry Department, Alexandria University, Egypt, conducted the cTnT assay (Roche Diagnostics, Mannheim, USA). Monoclonal antibodies against cTnT are used in the test (Zoheir et al., 2019).

Assay of Proinflammatory Cytokine

The cardiac homogenate was utilized to measure p53 (cat. no. ELR-p53-1; RayBiotech, INC.), interleukin-6 (IL-6; cat. no. ab100772), Vascular Endothelial Growth Factor(VEGF) (Ray Biotech, INC., Norcross, AG), and tumor necrosis factor-alpha (TNF-α; cat. no. ab100785) utilizing the corresponding ELISA kits (Abcam) by the directions provided by the supplier.

Histopathological Examination for Heart:

For histopathology, heart tissue sample was immersed within a 10% neutral buffered formalin solution. then were prepared for paraffin wax immersion, portions were sliced with a 5 mm thickness and dyed using Masson's trichrome and hematoxylin and eosin (H&E) (BaNCroft and AGmble, 2008). five distinct, non-overlapping sections from each animal investigated and analyzed using light microscope at (Anatomy Department, Zagazig University) and photographed.

Immunohistochemical Examination.

Sliced serial portions were placed on poly-lysine slide covers. Tissue slices are boiled in 10 mM citrate buffers PH 6.0 for ten to twenty minutes, and then cooled for 20 minutes at room temperature. phosphate-buffer saline (PBS) was used to wash the slides twice. The primary antibodies (1ry Ab) listed below have been utilized:

a) 0.1 ml of rabbit polyclonal 1ry Ab (Caspase3) diluted (Biovision, Milpitas Boulevard, Milpitas, CA 3015-100 Ab) (CA USA).

b) 0.1 ml at a concentrated 200 microgram (g)/ml 1ry Ab-l Ab (PCNA) (Labvision, USA).

For 60 minutes, the primary antibody was kept in a damp chamber at room temperature. The 1ry Ab used was diluted by 0.1 ml to lessen background and non-specific staining. Goat antipolyvalent that had been biotinylated was used, and it was kept in a moist chamber for 10 min at room temperature. The DAB chromogen mixture was kept at RT for five to fifteen min. For one to three minutes, Mayer Haematoxylin was used to counterstain the slides. Tonsils, which have a brown hue, are regarded as positive control specimens. For caspase3, the cellular location is the nucleus; for PCNA, the cytoplasm. However, in place of the principal antibody application step, a section of the heart muscle served to be a negative control (Abo Elfadl et al., 2017).

Image analysis.

Every rat within the various groups had 10 encoded fields across five sections, allowing for blind inspection and examination. Image J software (ImageJ/Fiji 1.46r, https://imagej.nih.gov/ij/index.html) was used for the examination of the images. Five randomly chosen fields from each Masson's trichrome stained segment were photographed at a 400x objective lens magnification to analyze the collagen in heart tissue and area% of caspase3 immuno-expression was detected from caspase 3 stained section. In addition, the total count of PCNA-positive cellular population (interstitial cells and vasculature smooth-muscle per area myocardial tissue as well as per vessel a cross-section luminal surface) was also counted (Amann et al., 1998).

Statistical analysis

The SPSS (Statistical Package for Social Science) version 26 program was used for statistical evaluation of all gathered biochemical and morphometric results. To confirm that the findings followed a pattern of normality and that the p-value was higher than 5%, the Shapiro-Wilk test was employed. For ease of display, data with normal distributions was summed using the mean and standard deviation. Consequently, the significance of the variation in the test groups' means was ascertained using the One-way ANOVA. For estimating various comparisons, the Tukey HSD post-hoc test was employed. A statistically significant value was defined as $p < 0.05$ at a degree of confidence of 95%.

Results & Discussion

Regarding histological and biochemical parameters, no significant statistical discrepancy was detected among positive control and negative control subgroups (Table 1).

Results of anthropometric measures

In relation to Body weight, no significant change ($p > 0.05$) in total body weight among all studied groups was detected except for the detected significant decline ($p < 0.05$) in rats received only high dose of ZnO-NPs versus positive control group. **Regarding heart weight,** a significant decline ($p < 0.05$) in rats' heart weights receiving both doses of ZnO-NPs when compared to both control subgroups. Coadministration of AG with the lower dosage of ZnO-NPs yielded a significant change ($p < 0.05$) in heart weight versus ZnO-NPs treated groups (at both low and high doses). On the other hand, administration of AG with high dose of ZnO-NPs implied a significant decline ($p < 0.05$) in heart weight versus both control subgroups and with only lower dosage of ZnO-NPs (table 1).

Table 1: Anthropometric measures analysis in different study groups

	Control group (n10)		**ZnO-NPs (n 20)**		**ZnO-NPs+ AG(n 20)**		
	NC subgroup (n10)	**PC subgroup (n10)**	**100 (n 10)**	**400(n 10)**	**100(n 10)**	**400(n 10)**	**P value**
Total body weight (BW) (gm)	***180±1.5***	***185±4***	***176.7±3.4***	***172.8±2 [b]***	***178.9±4***	***177.6±6***	***0.007***
Heart weight (HW) (gm)	***0.51±0.02***	***0.53±0.03***	***0.40±0.01 [a, b]***	***0.38±0.00 [a, b]***	***0.51±0.05 [c, d, f]***	***0.41±0.01 [a ,b ,e]***	***0.002 0.001***

One-way ANOVA, and Tukey HSD (post-hoc test), P > 0.05: no significant differences, P < 0.05: significant differences

a significant versus NC subgroup, b significant versus PC, c significant versus ZnO-NPs (100), d significant versus ZnO-NPs (400), e significant versus ZnO-NPs+ AG (100), f significant versus ZnO-NPs+ AG (400)

Biochemical results

Regarding levels of cardiac enzymes, low and high doses of ZnO-NPs treatment either alone or when co-administered with AG caused a significant rise ($p < 0.05$) in CK, LDH and troponin levels versus both control subgroups. When high dose of ZnO-NPs administered, there was a significant rise in both LDH and troponin when compared with ZnO-NPs low dose only. Co-treatment of AG with only high doses of ZnO-NPs yielded a significant change ($p < 0.05$) in level of CK and LDH when compared to both doses of ZnO-NPs. however, this significant change ($p < 0.05$) was detected with only low dose of ZnO- NPs when levels of troponin was estimated (table 2).

Table 2: cardiac enzymes analysis in different study groups

	Control group (n10)		**ZnO-NPs (n 20)**		**ZnO-NPs+ AG(n 20)**		
	NC subgroup (n10)	**PC subgroup (n10)**	**100(n 10)**	**400(n 10)**	**100(n 10)**	**400(n 10)**	**P value**
CK (u/L)	***970±20***	***968±12***	***1126.6±64 a, b***	***1270±20 a, b***	***1150±50 a ,b, f***	***1450±100 a, b, c, d, e***	***0.007***
LDH(IU)	***596.7±15***	***606±20***	***1100±50 a, b, d,***	***1213±15 a ,b ,c***	***1155±5 a, b, f***	***1310±10 a, b, c, d, e***	***0.000 0.001***
Troponin (Mg/ml)	***0.43±0.006***	***0.40±0.02***	***1.3±0.15 a, b, d,***	***1.7±0.15 a, b, c***	***1.5±0.11 a, b***	***1.6±0.12 a, b, c***	***0.00 0.030***

One-way ANOVA, and Tukey HSD (post-hoc test), P > 0.05: no significant differences, P < 0.05: significant differences **a significant versus NC subgroup, b significant versus PC, c significant versus ZnO-NPs (100), d significant versus ZnO-NPs (400), e significant versus ZnO-NPs+ AG (100), f significant versus ZnO-NPs+ AG (400)**

Regarding levels of inflammatory mediators:

In relation to il-6 levels: treatment with both doses of ZnO-NPs yielded a significant rise ($p < 0.05$) in il-6 versus both control subgroups. Co-adminstration of AG with low dose of ZnO-NPs, was accompanied with significantly change ($p < 0.05$) in level of il-6 versus positive control, both doses of ZnO-NPs and AG with high ZnO-NPs group. On the other hand, When AG was administered with higher dosage of ZnO-NPs, il6 level was significantly higher ($p < 0.05$) versus both control subgroups, high dose of ZnO-NPs and AG with low dose ZnO-NPs

group (table 3). **Regarding VEGF levels**: no significant change ($p > 0.05$) in VEGF levels among all studied groups was found except the significant increase ($p < 0.05$) in VEGF levels with higher ZnO-NPs dosage group versus positive control subgroup only (table 3). **Regarding TNF α levels** TNF α level rose significantly ($p < 0.05$) after treatment with both dosages of ZnO-NPs relative to both control subgroups. this was the same result obtained when AG was administered with high dose of ZnO-NPs (table 3). **Regarding P53 level:** treatment with both doses of ZnO-NPs either alone or if combined with AG yielded a significant rise ($p < 0.05$) in p53 levels versus both control subgroups. Co-administration of AG yielded a significant alteration ($p < 0.05$) when compared with both ZnO-NPs doses treated groups (table 3).

Table 3: inflammatory mediators' analysis in different study groups

	Control group (n10)		**ZnO-NPs (n 20)**		**ZnO-NPs+ AG(n 20)**		
	NC subgroup (n10)	**PC subgroup (n10)**	**100(n10)**	**400(n10)**	**100(n10)**	**400(n10)**	**P value**
IL-6 (pg/ml)	***27.1±1.2***	***25.67±1.1***	***34.3±1.2*** [a, b, d]	***46.5±2.3*** [a, b, c]	***29.6±1*** [b, c, d, f]	***34±0.7*** [a, b, d, e]	***0.000***
VEGF (pg/ml)	***205±15***	***185±15***	***221±35.5***	***248.3±15*** [b]	***226.7±15***	***233.3±12***	***0.019***
TNF α (pg/ml)	***233.3±35.1***	***216±15.8***	***313±32*** [a, b]	***380±36*** [a, b]	***283.3±15*** [d]	***330±17*** [a, b]	***0.008 0.000***
P53(ml/ng protein)	***4.2±1.5***	***3.9±0.1***	***9.9±0.4*** [a, b]	***14±0.2*** [a, b]	***7.8±0.3*** [a, b, c, d, f]	***11.9±0.1*** [a, b, c, d, e]	***0.000***

One-way ANOVA, and Tukey HSD (post-hoc test), P > 0.05: no significant differences, P < 0.05: significant differences

a significant versus NC subgroup, b significant versus PC, c significant versus ZnO-NPs (100), d significant versus ZnO-NPs (400), e significant versus ZnO-NPs+ AG (100), f significant versus ZnO-NPs+ AG (400)

Histological and Immunohistochemical results

Cardiac LM histological examination of control subgroups revealed healthy longitudinally organized cardiac muscle fibers. These fibers were either branching or anastomosing. Every myocardial cell possessed centralized vesicular nuclei and acidophilic cytoplasm (Fig. 1A& B). In the ZnO-NPs group (100, 400 mg/kg), The examination showed few disorganized muscle fibers with fibrosis either around blood vessels or in between myocardial cells along with increased cellular infiltrates. Some nuclei were fragmented. Vacuolation could be seen especially around nuclei (Fig. 1C& D). however, more widespread myocardial lesions have been observed in high doses (400 mg/kg) with multiple areas of necrosis which lodged areas of hemorrhage at some sites (Fig. 1D). On the other hand, in the Protected group, the combination with AG, resulted in a reduction in all histopathological abnormalities when compared to heart tissue from rats receiving ZnO-NPs (Fig. 1E & F).

Masson's trichrome dye was used to detect if there was any collagen deposited around muscle fibers. Sections of both control subgroups revealed sparse collagen fibers situated between myocardial fibers and around blood vessels (Fig. 2A, B). On the other hand, ZnO-NPs (100) treated group revealed moderate interstitial collagen fibers scattered either blood capillaries or in between muscle fibers (Fig. 2C). Furthermore, collagen fibers were seen in abundance in group ZnO-NPs (400) (Fig. 2D). However, AG+ ZnO-NPs (100) treated group displayed a minimal deposition of collagen fibers (Fig 2 E). AG+ ZnO-NPs (400) treated group showed moderate collagen fiber deposition (Fig 2F). After measuring the percentage of collagen area stained with Masson trichrome with immunohistochemistry, significantly higher levels of Masson trichrome stained area were detected in ZnO-NPs treated rats than did control ones ($p < 0.05$) and this rise was evident in high ZnO-NPs versus lower dosage. Comparing the co-administration of AG to the control or ZnO-NPs treated group revealed a substantial ($p < 0.05$) decline in the stained area when AG was administered with only high group (ZnO-NPs 400mg/kg). However, in low dose of ZnO-NPs with AG, this change was significant ($p < 0.05$) only against both doses of ZnO-NPs (Fig 2G).

Immunohistochemical staining with Caspase 3

Caspase-3 expression was not seen in cardiac tissue of control group (Fig. 3A &B). Whereas the ZnO-NP treated groups displayed a significant rise in caspase-3 level within cardiac cell cytoplasm with dark apoptotic nuclei. The inflammatory cells encircling necrotic muscle cells were heavily immunostained (Fig. 3C &D). The expression of activated caspase-3 appeared slightly reduced in AG-protected rats (Fig. 3E&F).

After measuring the caspase-3 activity degree with immunohistochemistry, significantly higher levels of expressed caspase-3 were detected in ZnO-NPs treated rats than did control ones ($p < 0.05$) and this rise was evident also between the 2 tested doses of ZnO-NPs. Comparing the co-administration of AG to the control or ZnO-NPs treated group revealed a substantial ($p < 0.05$) alteration in the caspase 3positive stained area (Fig 3G).

Immunohistochemical staining with PCNA

In the heart muscle fibers of control group, PCNA expression was modest (Fig. 4 A&B). Conversely, ZnO-NPs treatment significantly reduced PCNA expression in heart muscle fibers (Fig. 4 C&D). Fortunately, AG administration increased PCNA expression in heart muscle fibers much more than ZnO-NPs alone (Fig. 4E&F). Rats subjected to ZnO-NPs showed significantly lower PCNA expression ($p < 0.05$) than control animals, according to a quantitative immunohistochemistry analysis (Fig. 4G). Co administration of AG yielded a substantial difference ($p < 0.05$) versus ZnO-NPs treatment group and control group (Fig. 4G).

Physiological results

Assessment of ECG parameters

Rats of control group displayed normal ECG pattern with normal QRS complex, normal P-R interval and normal heart rate (Fig. 5A&B). On the other hand, abnormal ECG pattern in ZnO-NPs treated group was detected. There was a decreased QRS complex amplitude, shortened time of P-R interval and increased heart rate (Fig. 5C). These abnormalities were more evident in high dose treated rats (Fig. 5D). When AG combined with ZnO-NPs, ECG pattern returned to normal; QRS complex, P-R interval and heart rate were closely normal with low ZnO-NPs dose (Fig. 5 E) and was near to normal with high dose (Fig. 5 F).

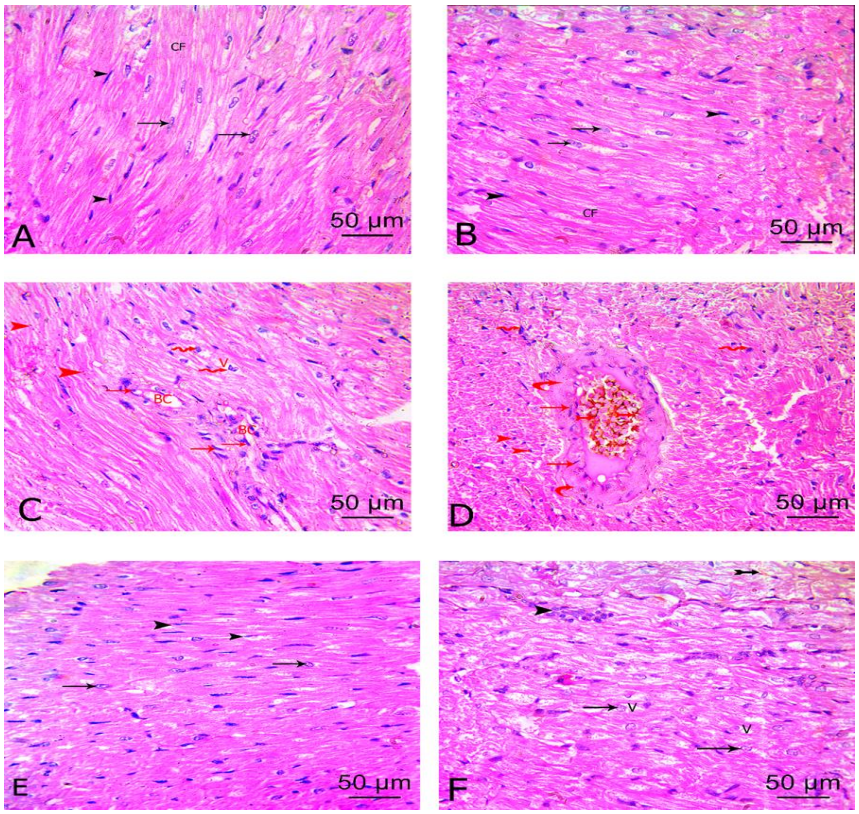

Fig. 1*:* H&E stained sections of adult male albino rat cardiac muscle of different studied groups; Negative control(A), Positive control (B), ZnO-NPs (100mg) treated group (C), ZnO-NPs (400mg) treated group (D), Arabic Gum (AG)+ ZnO-NPs (100mg) group (E) and Arabic Gum (AG)+ ZnO-NPs (400mg) (F) at 400x magnifications. (A & B): displaying longitudinally organized cardiac muscle fibers with acidophilic cytoplasm central vesicular oval nuclei

(arrows) along with longitudinal and transverse cardiac fiber striations (CF). These fibers are anastomosing and branching off of one another with densely flattened connective tissue nuclei (arrow heads) present in these cells. (C& D): displaying myocytes disarray with condensed or irregular fragmented nuclei (red wavy arrow). Some inflammatory cells (red arrow heads) are seen in between the muscle fibers, also there was Perivascular fibroblasts (red arrows) around blood capillaries (red BC) seen in-between muscle fibers and vacuolations (red V) especially around the nuclei. In addition to wide areas of myocytes necrosis (red curved arrows) with central areas of hemorrhage (red double head arrow) which are seen obviously in (D). (E): displaying most of myocytes are more or less as the control group. The nuclei are more or less as the control (arrow). Some fibroblasts are seen (arrow head). (F): displaying the majority of myocytes are similar to the control group. The nuclei are similar to the control (arrow) with some vacuolations (V) around it however there is some cellular infiltration (arrow head). (H&E X400), (scale Bar 50).

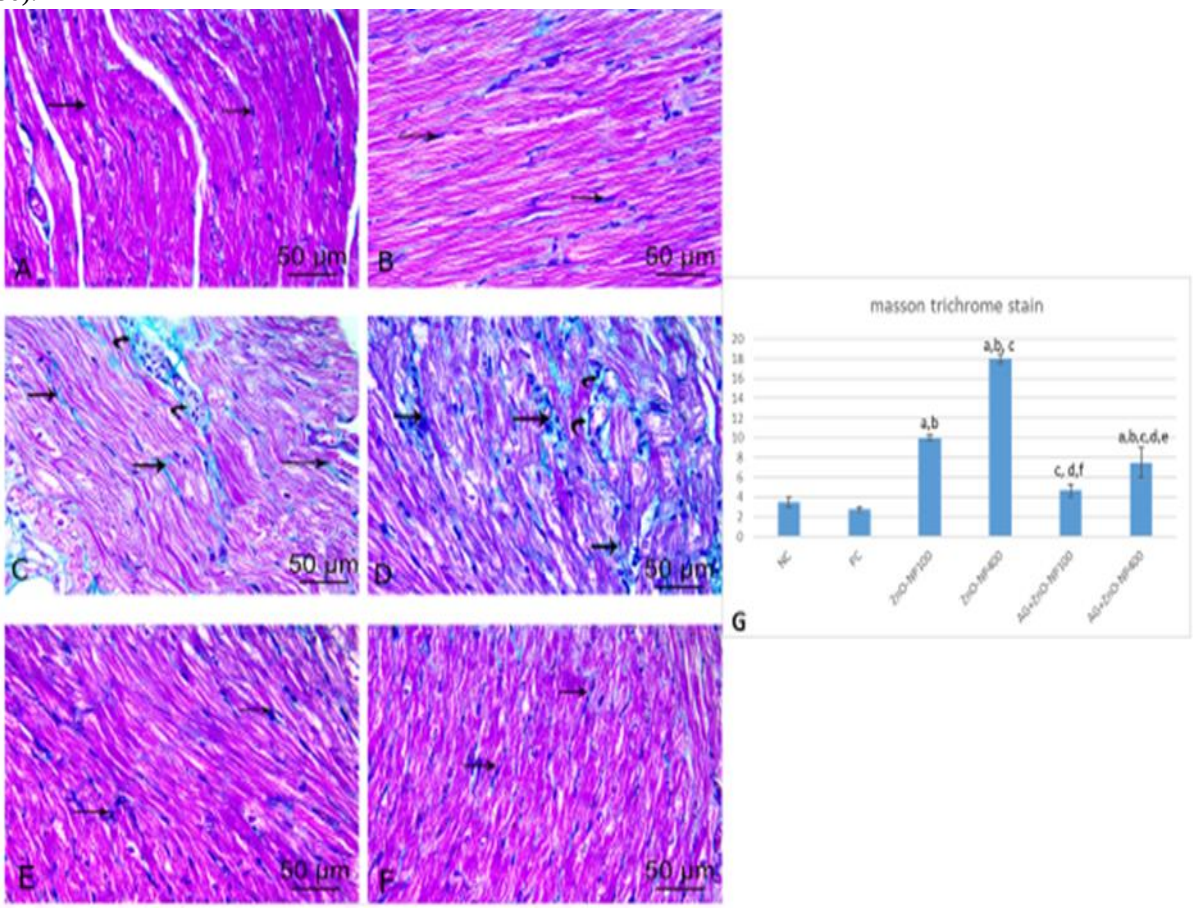

Fig. 2: Masson's trichrome stained sections of adult male albino rat cardiac muscle of different studied groups at 400x magnifications; Negative control(A), Positive control (B), ZnO-NPs (100mg) treated group (C), ZnO-NPs (400mg) treated group (D), Arabic Gum(AG)+ ZnO-NPs (100mg) group (E) and Arabic Gum(AG)+ ZnO-NPs (400mg) (F). (A & B): displaying normal cardiac muscle with minimal interstitial fibrosis in-between muscle fibers (arrows). (C, D): displaying cardiac muscles with marked fibrosis either perivascular (curved arrow) or interstitial fibrosis between muscle fibers (arrows). This fibrosis was extensive in (D). (E): displaying normal cardiac muscle with minimal interstitial fibrosis in-between muscle fibers (arrows). (F): displaying normal cardiac muscle with minimal to moderate interstitial fibrosis in-between muscle fibers (arrows). (G): Chart shows morphometrical analysis of area percentage of collagen fibers between different studied group. (Masson's trichrome X400), (scale Bar 50).

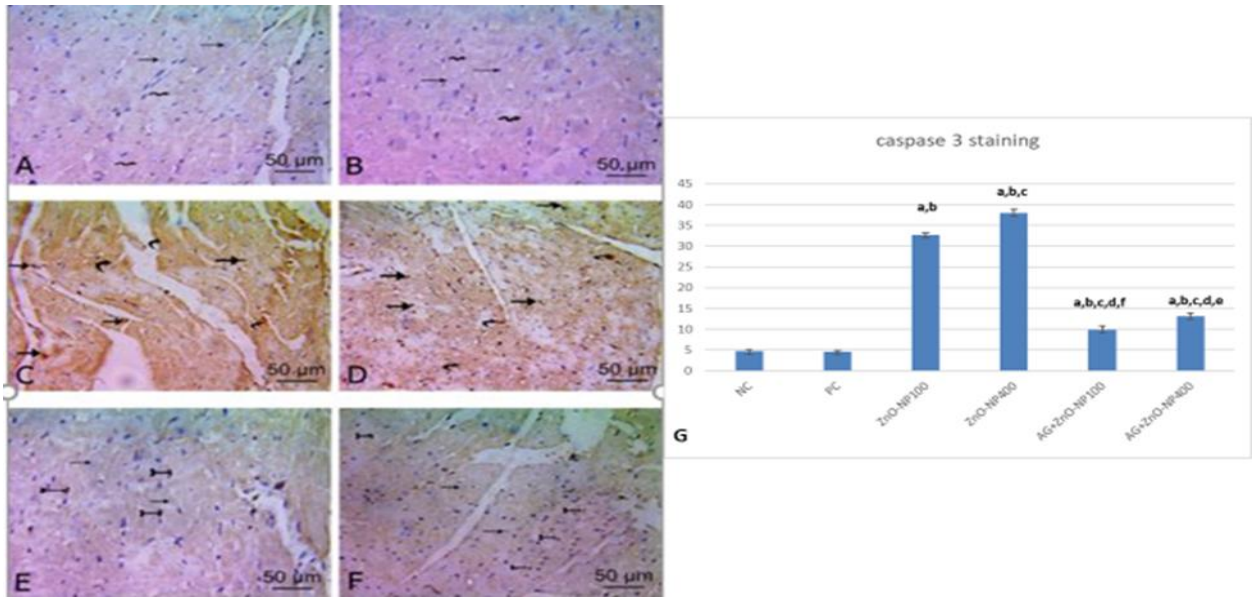

Fig. 3: Caspase- 3 stained sections of adult male albino rat cardiac muscle of different studied groups at 400x magnifications; Negative control(A), Positive control (B), ZnO-NPs (100mg) treated group (C), ZnO-NPs (400mg) treated group (D), Arabic Gum (AG)+ ZnO-NPs (100mg) group (E) and Arabic Gum (AG)+ ZnO-NPs (400mg) (F). (A, B) displaying no nuclear (arrows) or cytoplasmic (wavy arrows) immune reaction for caspase -3. (C): displaying marked cytoplasmic (curved arrow) and nuclear (thick arrow) caspase -3 reaction. (D): displaying excessive cytoplasmic (curved arrow) and nuclear (thick arrow) caspase -3 reaction. (E): displaying mild cytoplasmic and nuclear caspase -3 reaction: some nuclei show positive reaction (double head arrow) and others show negative reaction (arrow). (F): displaying moderate cytoplasmic and nuclear caspase -3 reaction: some nuclei show positive reaction (double head arrow) and others show negative reaction (arrow). (G): Chart shows morphometrical analysis of caspase-3 positive stained area percentage between different studied group. (Caspase 3 X400), (scale Bar 50).

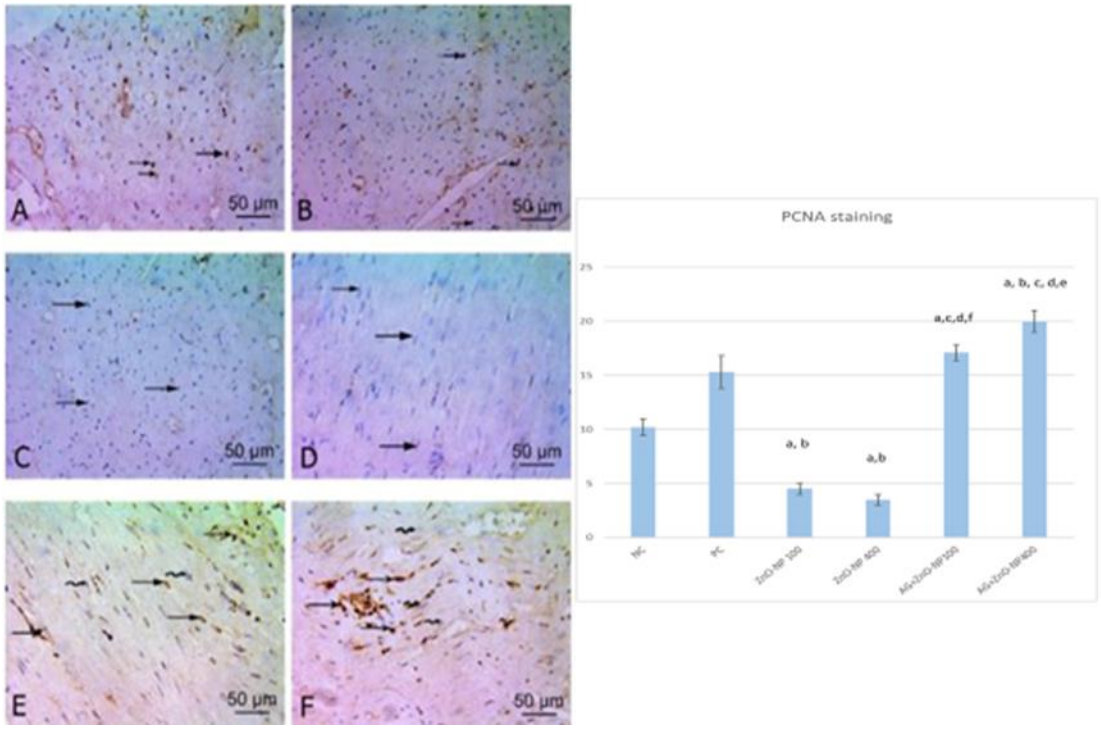

Fig. 4: PCNA stained sections of adult male albino rat cardiac muscle of different studied groups at 400x magnifications; negative control(A), Positive control (B), ZnO-NPs (100mg) treated group (C), ZnO-NPs (400mg)

treated group (D), Arabic Gum (AG)+ ZnO-NPs (100mg) group (E) and Arabic Gum (AG)+ ZnO-NPs (400mg) (F). (A, B) displaying strong positive nuclear reaction (arrows) for PCNA immunostaining. (C, D): displaying no nuclear reaction (arrow) for PCNA immune staining. (E): displaying mild nuclear reaction for PCNA immune staining, some nuclei show mild brownish discoloration (arrow) and others show negative reaction (wavy arrow) (F): displaying marked reaction for PCNA immune staining, some nuclei show dark brownish discoloration (arrow) and others show negative reaction (wavy arrow) (G): Chart shows morphometrical analysis of PCNA positive stained cells between different studied group. (PCNA X400), (scale Bar 50).

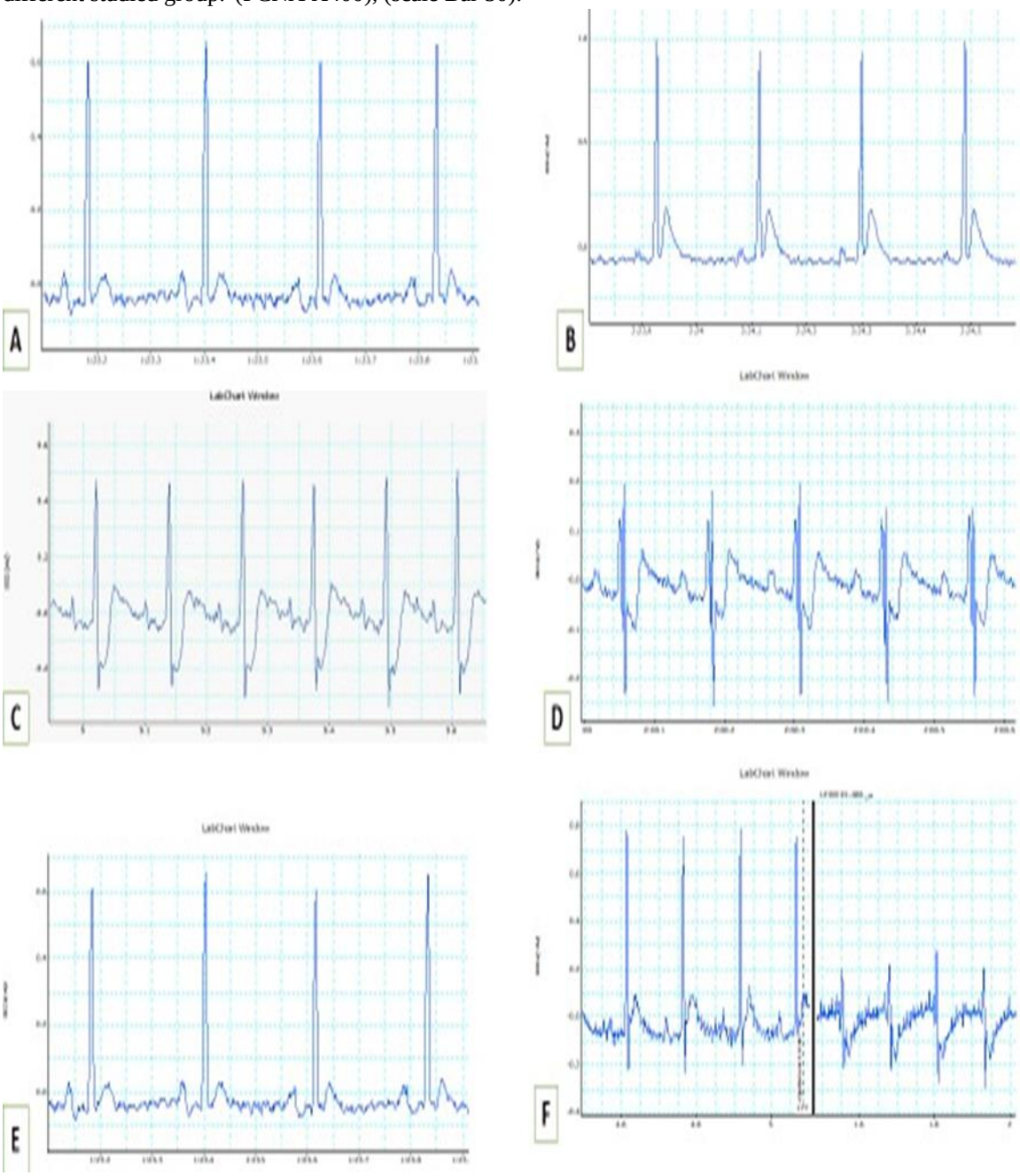

Fig 5: ECG pattern of different studied groups: negative control(A), Positive control (B), ZnO-NPs (100mg) treated group (C), ZnO-NPs (400mg) treated group (D), Arabic Gum (AG)+ ZnO-NPs (100mg) group (E) and Arabic Gum (AG)+ ZnO-NPs (400mg) (F). Control group showed normal ECG with normal QRS complex, normal P-R interval (A&B). ZnO-NPs treated rats yielded decreased QRS complex amplitude, shortened time of P-R interval (C&D). AG improved ECG pattern and returned it near normal (E& F).

Discussion

The body's exposure to ZnO nanoparticles grows with increased use. Aspiration, dermatological contact, and ingesting are the most common routes for ZnO nanoparticle exposure. The cardiovascular system is the primary body region exposed to ZnO-NPs in some way. The pulmonary, hepatic and renal tissues are principal sites of ZnO nanoparticles and contain enormous compatibility (Iavicoli et al., 2017). Several recent investigations demonstrated the toxicity of ZnO-NPs on various tissue and cellular types. The high dissolution rate of the particles was blamed for the harmful effects, which included cytotoxicity, oxidative damage, and damage to mitochondria (Condello et al., 2016).

In this study, a substantial decrease in rat body weights were obviously detected only with ZnO-NPs 400mg/kg. On the contrary to this result, (Hong et al., 2014) found the body weight losses were evident with even low doses of ZnO-NPs in a research using rats administered various dosages of ZnO-NPs (0, 100, 200, and 400 mg/kg/day) via oral route and explained that it might be as a result of reduced food intake. On the other hand, (Wang et al., 2016) demonstrated that nanoZnOs at doses of 50 & 500 mg/kg was accompanied with body weight rise whereas those at 5000 mg/kg demonstrated losses in it. These results are obvious signs of the generalized harm generated by ZnO-NPs and imply that its consumption causes minor anorexia followed by decreased total weight gains in rat.

On the other hand, this study's results demonstrated that, administration of different doses of ZnO-NPs yielded significant declined heart weights versus control group which was consistent with findings of (Yousef et al., 2022) in a previous research investigating effect of both aluminum oxide (Al_2O_3-NPs) and 100 mg zinc oxide (ZnO-NPs) either individually or combined on rat heart, lung and brain. However, this didn't match results of (Ko et al., 2015) in rats fed with 100 mg ZnO NPs which may be as a consequence of short duration of exposure. The previous authors exposed rats for 2 weeks only.

Oxidative distress was recently identified as a major contributor to ZnO-NP cytotoxicity (Tang et al., 2018). When ZnO-NPs enter tissues, they activate a defensive process that creates ROS that exceeds antioxidant defenses, thereby resulting in an inflammatory reaction that damages the mitochondrial electron transport chain at its inner membranes as well as cellular elements including DNA, resulting in the breakdown of cells and their deaths (Ghosh et al., 2016). So this study searched levels of inflammatory cytokines and reported that; ZnO-NPs increased production of IL-6, TNF-, p53 and VEGF. This was similar to what was reported by (Yan et al., 2017) to describe the adverse cardiovascular outcomes generated by ZnO-NPs in vitro and in vivo.

Previous authors found increased inflammatory cytokines IL-8 and TNF- production within Broncho-alveolar lavage of ZnO-NPs-treated rats in a dose-related way. ZnO-NPs were found to stimulate the generation of inflammatory mediators by endocytosis in the in vitro experiments. TNF-, p53, and IL-6 levels in rat cardiac cells rose as a consequence of ZnO-NP administration, a result that is similar to (Wu et al., 2010) and (Tang et al., 2016). TNF- has been identified as a frequent inflammatory chemokine and immunologic indicator that

arises in response to ZnO and other metal oxide toxicities (D'Alessandris et al., 2007). It promotes inflammation in tissues by stimulating the generation of IL-6 along with additional cytokines that contribute to inflammation (Kerner et al., 2005). In this regard, (Yousef et al., 2022) reported that Al_2O_3-NPs and ZnO-NPs, either separately or if combined, may boost cytokines (IL-6 and TNF).

P53 is the major apoptotic controller. As a result, previous researches looked at the production of the tumor suppressor protein p53 to see if it was related to ZnO's DNA-damaging capability (Tesniere et al., 2008). In this research, P53 levels were elevated in ZnO-NP treated heart cells. Matching with this finding, (Ng et al., 2011) stated that ZnO-NPs induced the p53 pathways, that's primarily triggered by oxidative damage and (Han et al., 2016) added that ZnO-NPs stimulated cellular toxicity is influenced by dosage and duration. The tumor regulator protein p53, a key biological stress sensor, may induce the stoppage of the cell cycle and apoptosis (Zhang et al., 2016).

Cardiac enzymes (CK and LDH) are generally found within myocardial cells. The distribution of such enzymes produced by cells in the blood reflects changes in the health of plasma membranes as well as its permeability (Yousef et al., 2019). In agreement with this, both doses of ZnO-NPs in this study were accompanied with a substantial elevation in CK versus control groups. This matched results of (Ko et al., 2015) in male Sprague-Dawley rats intoxicated by different doses of ZnO-NPs for 2 weeks.

Alterations in cardiovascular morphology were indicative of ZnO-NPs' damage to the cardiovascular system. ZnO-NPs treatment in the current study resulted in varied cardiac histopathological alterations, disrupted muscle fibers, and increased cellular infiltrates, that may be attributed primarily to enhanced eosin adsorption to the denatured cytoplasmic proteins as implied by (Zoheir et al., 2019) in rats. Also, some pathological features were also evident as cellular necrosis along with vacuolar degeneration which was in harmony with results of (Moshrefi et al., 2021) in a research using different doses of ZnO-NPs and emphasized these alterations to be dose-dependent.

In the current study, Masson trichrome stain results demonstrated that the heart tissues of rats subjected to ZnO-NPs presented more collagen deposition exceeding that of control groups, this was in harmony with (Herrera-Rodríguez et al., 2023) who stated that collagen deposition reflects a fibrotic response caused by past chronic inflammatory responses and added that cardiac fibrosis can result in organ damage and even mortality.

Jacobsen and colleagues discovered that animals treated to NM-111 ZnO- NPs via oro-pharyngeal administration exhibited elevated lung collagen buildup (fibrosis) (Jacobsen et al., 2015). (Azad et al., 2013) stated that, another factor contributing to the toxicity of NPs is ROS-mediated stimulation of fibrogenesis. In this context, results of this study implied a rise in generation of all pro-inflammatory mediators (TNF and IL-6 release) which was linked to the presence of cells associated with inflammation and subsequent fibrosis noticed in heart tissue of rats which received ZnO-NPs. Also (Senapati et al., 2015, Roy et al., 2014) emphasized the ability of ZnO-NPs to elevate mediators of inflammation and ROS in vitro

(THP-1 cell, blood cell, macrophage cells) as well as in vivo (rodents) confirming the idea that NPs could result in responses of inflammatory nature (Liang et al., 2018, Hendy and Canaff, 2016).

In this study, statistical analysis of caspase 3 morphometry showed increased positive area percentage of caspase 3 in ZnO-NPs treated rats. Previously, (Choudhury et al., 2017) proved that ZnO-NP consumption induced the production of apoptosis-related genes and noted an increase in Caspase-3 expression. (Roberge et al., 2014) associated Caspase-3 activity with the production of apoptosis and myofibril breakdown and stated that Caspase-3 can trigger the breakdown of heart myofibrillar protein. (Herrera-Rodríguez et al., 2023) established that ZnO-NPs cytotoxicity is connected with the generation of ROS and proved that in mitochondria of rodent's cardiac tissue following being exposed to NPs. Maintaining the activity of mitochondria seems essential to guaranteeing that ATP reaches the subcellular and cellular processes which are dependent upon it (Zazueta et al., 2018). Imbalances in the utilization of oxygen and ATP generation impair energy supply as well as permeable membranes with resultant cytosolic release of protein produced by mitochondria, such as Cyt-C, which triggers heart apoptosis and programmed death cascades (Chistiakov et al., 2018).

ZnO-NPs impacts upon cellular proliferation was detected by PCNA immunostaining since PCNA is thought to have a function in cell cycle mechanics and is thus a helpful indicator for cell proliferation (Zerjatke et al., 2017). This study showed a substantial decline in PCNA stained cells of ZnO-NP subjected rats. In agreement of these findings, (Sharma et al., 2011) treated human stomach adenocarcinoma with ZnO-NPs and a considerable suppression of cell growth was detected. ZnO-NPs seemed to trigger cytotoxicity through oxidation with destruction of growing tissue more selectively than healthy one (Abass et al., 2017).

The impact of ZnO-NPs upon ECG parameters were assessed during the present research. It was discovered that ZnO-NPs raised heart rate, dramatically shortened P-R intervals times, and reduced QRS complex magnitude at all doses. These results make sense because excess zinc ions can alter the electrical activity of cardiomyocytes (Turan and TuNCay, 2017) and zinc acts a crucial part in the interaction of excitation and contraction in mammalian cardiomyocytes(Turan and TuNCay, 2017). Furthermore, it was discovered that rats' serum calcium content may be raised by ZnO-NPs. Therefore, variations in calcium levels or the release of zinc ions from ZnO-NPs may impact the electrical functioning of cardiomyocytes and alter ECG characteristics including the P-R interval (Torabi et al., 2018).

Arabic gum is typically utilized throughout the Middle East and North Africa to treat a variety of conditions, such as kidney failure, liver failure, heart failure, anemia, and type 2 diabetes (Zeid and FarajAllah, 2018). The AG preventive impacts seem to be due to being anti-inflammatory and anti-oxidative (Hammad et al., 2019). Arabic gum is an antioxidant that protects against drug-induced cardiotoxicity (Abd-Allah et al., 2002). It has also been used for the management of a variety of disorders, involving heart problems (Glover et al., 2009).

In this study, the histopathological examination of the group receiving (AG &ZnO-NPs) treatment revealed similar myocardial histology as the control groups. As a consequence, when AG was combined with ZnO-NPs, the myocardium was considerably preserved which was demonstrated via results of Pathological examinations which support AG's cardiac protection. This impact of AG may be related to its powerful anti-oxidant and free radical-neutralizing properties (Elderbi et al., 2014). Also ZnO-NPs increased cardiac apoptosis that was revealed by caspase 3 staining of this study and this impact was improved by AG. Previously (Savitskaya and Onishchenko, 2015) stated that the stimulation of caspase-3 by reactive oxygen species can result in apoptosis, and that AG administration can counteract this effect. The activation of particular proteases, such as caspases3, is a key mechanism of apoptosis (Zhang et al., 2019). Drug therapy with AG exhibited a strong inhibitory effect on the up-regulation of this gene in rats. This could be due to AG's anti-apoptotic properties (Moustafa et al., 2014).

Results of this study implied that AG treatment considerably reduced generation of TNF and IL-6 that can be induced by ZnO-NPs administration as was previously demonstrated by (Nemmar et al., 2019) in mice produced by water pipe smoke. AG appears to be a powerful natural anti-inflammatory and antioxidant agent. Current study results support earlier therapeutic and experimental investigations suggesting that AG exerts anti-oxidant properties in sickle-cell anemic patients as along with the anti-inflammatory and antioxidant capabilities in animals suffering from prolonged kidney dysfunction (Za'abi et al., 2018, Kaddam et al., 2017). Also (Gouda and Babiker, 2022) reported that AG defends cardiac tissue by acting as an antioxidant and anti-inflammatory and eventually reduced pro-inflammatory cytokine production (Gouda and Babiker, 2022).

Also, AG improved to some extent the cardiac enzymatic levels indicating a positive impact upon myocardium. CK and LDH levels were restored in animals that had concomitantly received AG therapy as was detected by (Elderbi et al., 2014).

Furthermore, AG ameliorates the ECG pattern getting it to be so closely to the normal pattern. The results presented here line up with the findings of Fouda et al., whose work suggested that AG has a moderating influence on ECG (Fouda et al., 2019). AG's ability to raise antioxidant elements including copper, iron and manganese as well as its favorable impact on the production of enzymes that protect against damage, can account for this benefit (Kong et al., 2014).

Conclusion

It appears that ZnO nanoparticles can result in histological and biochemical alteration for heart tissue along with abnormal ECG characteristics in rats, most likely through production of reactive oxygen species with increment of inflammatory mediators and this effect worsened by increasing dose. Furthermore, AG may have a protective impact on the heart muscle produced by ZnO-NPs. However, more research still is needed to illustrates the mechanisms of cardiac injury produced by ZnO-NPs.

Statements & Declarations

Funding

"The authors declare that no funds, grants, or other support were received during the preparation of this manuscript."

Competing Interests

"The authors have no relevant financial or non-financial interests to disclose."

Author Contributions

"All authors contributed to the study conception and design. Material preparation, data collection and analysis were performed by [full name], [full name] and [full name]. The first draft of the manuscript was written by [full name] and all authors commented on previous versions of the manuscript. All authors read and approved the final manuscript.

Acknowledgement

With special gratitude to the human anatomy and embryology department at Zagazig University's Faculty of Medicine. Much regards to the Scientific Medical Research Center and the Animal House Department of Zagazig University.

Author contributions

Each writer took part in the actual effort that produced the work, and they will all take responsibility for its content both individually and jointly.

Funding Statement: None

Declaration of interests: None

References:

ABASS, M. A., SELIM, S. A., SELIM, A. O., EL-SHAL, A. S. & GOUDA, Z. A. 2017. Effect of orally administered zinc oxide nanoparticles on albino rat thymus and spleen. IUBMB life, 69, 528-539.

ABD-ALLAH, A. R., AL-MAJED, A. A., MOSTAFA, A. M., AL-SHABANAH, O. A., DIN, A. G. E. & NAGI, M. N. 2002. Protective effect of arabic gum against cardiotoxicity induced by doxorubicin in mice: a possible mechanism of protection. Journal of biochemical and molecular toxicology, 16, 254-259.

ABO ELFADL, S., SHENDI, M., REDA, A. & ABDELHALEEM, A. 2017. Resveratrol pre-and post-treatment in doxorubicin-induced cardiac injury in relation to endogenous stem cell activation. Journal of Medical Histology, 1, 19-29.

AL-DOAISS, A. A. & AL-SHEHRI, M. A. 2020. Protective Effect of Gum Arabic/Insulin Against Histological Changes in Testes of Diabetic Rats. International Journal of Morphology, 38.

AL ZA'ABI, M., AL SALAM, S., AL SULEIMANI, Y., MANOJ, P., NEMMAR, A. & ALI, B. H. 2018. Gum acacia improves renal function and ameliorates systemic inflammation, oxidative and nitrosative stress in streptozotocin-induced diabetes in rats with adenine-induced chronic kidney disease. Cellular Physiology and Biochemistry, 45, 2293-2304.

ALI, B. H., ZIADA, A. & BLUNDEN, G. 2009. Biological effects of gum arabic: a review of some recent research. Food and chemical Toxicology, 47, 1-8.

AMANN, K., KRONENBERG, G., GEHLEN, F., WESSELS, S., ORTH, S., MÜNTER, K., EHMKE, H., MALL, G. & RITZ, E. 1998. Cardiac remodelling in experimental renal failure--an immunohistochemical study. Nephrology, dialysis, transplantation: official publication of the European Dialysis and Transplant Association-European Renal Association, 13, 1958-1966.

AZAD, N., IYER, A. K. V., WANG, L., LIU, Y., LU, Y. & ROJANASAKUL, Y. 2013. Reactive oxygen species-mediated p38 MAPK regulates carbon nanotube-induced fibrogenic and angiogenic responses. Nanotoxicology, 7, 157-168.

BAKHET, M. S. A. 2007. SERUM ACTIVITY OF CREATINE PHOSPHO-KINASE ENZYME AND UREA/CREATININE SERUM LEVEL IN UNCONTROLLED DIABETIC PATIENTS TYPE 2 WITH ACUTE ONSET OF SPONTANEOUS MUSCLE PAIN. AAMJ, 5.

BANCROFT, J. D. & GAMBLE, M. 2008. Theory and practice of histological techniques, Elsevier health sciences.

BÉNÉTEAU-BURNAT, B. & BAUDIN, B. 1991. Angiotensin-converting enzyme: clinical applications and laboratory investigations on serum and other biological fluids. Critical reviews in clinical laboratory sciences, 28, 337-356.

CHISTIAKOV, D. A., SHKURAT, T. P., MELNICHENKO, A. A., GRECHKO, A. V. & OREKHOV, A. N. 2018. The role of mitochondrial dysfunction in cardiovascular disease: a brief review. Annals of medicine, 50, 121-127.

CHOUDHURY, S. R., ORDAZ, J., LO, C.-L., DAMAYANTI, N. P., ZHOU, F. & IRUDAYARAJ, J. 2017. From the cover: zinc oxide nanoparticles-induced reactive oxygen species promotes multimodal cyto-and epigenetic toxicity. Toxicological sciences, 156, 261-274.

CONDELLO, M., DE BERARDIS, B., AMMENDOLIA, M. G., BARONE, F., CONDELLO, G., DEGAN, P. & MESCHINI, S. 2016. ZnO nanoparticle tracking from uptake to genotoxic damage in human colon carcinoma cells. Toxicology in Vitro, 35, 169-179.

D'ALESSANDRIS, C., LAURO, R., PRESTA, I. & SESTI, G. 2007. C-reactive protein induces phosphorylation of insulin receptor substrate-1 on Ser 307 and Ser 612 in L6 myocytes, thereby impairing the insulin signalling pathway that promotes glucose transport. Diabetologia, 50, 840-849.

ELDERBI, M. A., MOHAMED, A.-W. H., HADI, A.-H. A. & DABOBASH, M. D. 2014. Potential protective effect of gum Arabic against doxorubicin-induced Cardiotoxicity in Wistar albino rats. International Journal of Pharmaceutical Sciences and Research, 5, 1023.

ESMAEILLOU, M., MOHARAMNEJAD, M., HSANKHANI, R., TEHRANI, A. A. & MAADI, H. 2013. Toxicity of ZnO nanoparticles in healthy adult mice. Environmental toxicology and pharmacology, 35, 67-71.

FOUDA, A., EL-AZIZ, A. & MABROUK, N. 2019. Effects of Arabic Gum on cardiomyopathy in a rat model of type II diabetes. Al-Azhar Medical Journal, 48, 29-42.

GHOSH, M., JANA, A., SINHA, S., JOTHIRAMAJAYAM, M., NAG, A., CHAKRABORTY, A., MUKHERJEE, A. & MUKHERJEE, A. 2016. Effects of ZnO nanoparticles in plants: cytotoxicity, genotoxicity, deregulation of antioxidant defenses, and cell-cycle arrest. Mutation Research/Genetic Toxicology and Environmental Mutagenesis, 807, 25-32.

GLOVER, D. A., USHIDA, K., PHILLIPS, A. O. & RILEY, S. G. 2009. Acacia (sen) SUPERGUM™(Gum Arabic): an evaluation of potential health benefits in human subjects. Food Hydrocolloids, 23, 2410-2415.

GOUDA, E. & BABIKER, F. 2022. Gum Arabic protects the rat heart from ischemia/reperfusion injury through anti-inflammatory and antioxidant pathways. Scientific Reports, 12, 17235.

HAMMAD, F. T., AL SALAM, S., NEMMAR, A., ALI, M. & LUBBAD, L. 2019. The effect of arabic gum on renal function in reversible unilateral ureteric obstruction. Biomolecules, 9, 25.

HAN, Z., YAN, Q., GE, W., LIU, Z.-G., GURUNATHAN, S., DE FELICI, M., SHEN, W. & ZHANG, X.-F. 2016. Cytotoxic effects of ZnO nanoparticles on mouse testicular cells. International journal of nanomedicine, 5187-5203.

HENDY, G. N. & CANAFF, L. Calcium-sensing receptor, proinflammatory cytokines and calcium homeostasis. Seminars in cell & developmental biology, 2016. Elsevier, 37-43.

HERRERA-RODRÍGUEZ, M. A., DEL PILAR RAMOS-GODINEZ, M., CANO-MARTÍNEZ, A., SEGURA, F. C., RUIZ-RAMÍREZ, A., PAVÓN, N., LIRA-SILVA, E., BAUTISTA-PÉREZ, R., THOMAS, R. S. & DELGADO-BUENROSTRO, N. L. 2023. Food-grade titanium dioxide and zinc oxide nanoparticles induce toxicity and cardiac damage after oral exposure in rats. Particle and Fibre Toxicology, 20, 1-16.

HONG, J.-S., PARK, M.-K., KIM, M.-S., LIM, J.-H., PARK, G.-J., MAENG, E.-H., SHIN, J.-H., KIM, M.-K., JEONG, J. & PARK, J.-A. 2014. Prenatal development toxicity study of zinc oxide nanoparticles in rats. International Journal of Nanomedicine, 9, 159-171.

IAVICOLI, I., LESO, V., BEEZHOLD, D. H. & SHVEDOVA, A. A. 2017. Nanotechnology in agriculture: Opportunities, toxicological implications, and occupational risks. Toxicology and applied pharmacology, 329, 96-111.

JACOBSEN, N. R., STOEGER, T., VAN DEN BRÛLE, S., SABER, A. T., BEYERLE, A., VIETTI, G., MORTENSEN, A., SZAREK, J., BUDTZ, H. C. & KERMANIZADEH, A. 2015. Acute and subacute pulmonary toxicity and mortality in mice after intratracheal instillation of ZnO nanoparticles in three laboratories. Food and Chemical Toxicology, 85, 84-95.

JARRAR, A. H., STOJANOVSKA, L., APOSTOLOPOULOS, V., FEEHAN, J., BATAINEH, M. A. F., ISMAIL, L. C. & AL DHAHERI, A. S. 2021. The effect of gum arabic (Acacia senegal) on cardiovascular risk factors and gastrointestinal symptoms in adults at risk of metabolic syndrome: A randomized clinical trial. Nutrients, 13, 194.

KADDAM, L., FADL-ELMULA, I., EISAWI, O. A., ABDELRAZIG, H. A., SALIH, M. A., LANG, F. & SAEED, A. M. 2017. Gum Arabic as novel anti-oxidant agent in sickle cell anemia, phase II trial. BMC hematology, 17, 1-6.

KAO, Y.-Y., CHEN, Y.-C., CHENG, T.-J., CHIUNG, Y.-M. & LIU, P.-S. 2012. Zinc oxide nanoparticles interfere with zinc ion homeostasis to cause cytotoxicity. Toxicological Sciences, 125, 462-472.

KERNER, A., AVIZOHAR, O., SELLA, R., BARTHA, P., ZINDER, O., MARKIEWICZ, W., LEVY, Y., BROOK, G. J. & ARONSON, D. 2005. Association between elevated liver enzymes and C-reactive protein: possible hepatic contribution to systemic inflammation in the metabolic syndrome. Arteriosclerosis, thrombosis, and vascular biology, 25, 193-197.

KIM, K.-M., KIM, T.-H., KIM, H.-M., KIM, H.-J., GWAK, G.-H., PAEK, S.-M. & OH, J.-M. 2012. Colloidal behaviors of ZnO nanoparticles in various aqueous media. Toxicology and Environmental Health Sciences, 4, 121-131.

KO, J.-W., HONG, E.-T., LEE, I.-C., PARK, S.-H., PARK, J.-I., SEONG, N.-W., HONG, J.-S., YUN, H.-I. & KIM, J.-C. 2015. Evaluation of 2-week repeated oral dose toxicity of 100 nm zinc oxide nanoparticles in rats. Laboratory animal research, 31, 139-147.

KONG, H., YANG, J., ZHANG, Y., FANG, Y., NISHINARI, K. & PHILLIPS, G. O. 2014. Synthesis and antioxidant properties of gum arabic-stabilized selenium nanoparticles. International journal of biological macromolecules, 65, 155-162.

LI, C.-H., SHEN, C.-C., CHENG, Y.-W., HUANG, S.-H., WU, C.-C., KAO, C.-C., LIAO, J.-W. & KANG, J.-J. 2012. Organ biodistribution, clearance, and genotoxicity of orally administered zinc oxide nanoparticles in mice. Nanotoxicology, 6, 746-756.

LIANG, H., CHEN, A., LAI, X., LIU, J., WU, J., KANG, Y., WANG, X. & SHAO, L. 2018. Neuroinflammation is induced by tongue-instilled ZnO nanoparticles via the Ca2+-dependent NF-κB and MAPK pathways. Particle and fibre toxicology, 15, 1-21.

LIU, J., FENG, X., WEI, L., CHEN, L., SONG, B. & SHAO, L. 2016. The toxicology of ion-shedding zinc oxide nanoparticles. Critical reviews in toxicology, 46, 348-384.

MAHDAVI, S. A., JAFARI, S. M., ASSADPOOR, E. & DEHNAD, D. 2016. Microencapsulation optimization of natural anthocyanins with maltodextrin, gum Arabic and gelatin. International journal of biological macromolecules, 85, 379-385.

MOSHREFI, A., HOSSEINI, S. & PARVIZI, M. 2021. Toxicological effect of exposure to different doses of zinc oxide nanoparticles on brain and heart structures of male WIstar rats. Bulg J Vet Med. https://doi. org/10.15547/bjvm, 50.

MOUSTAFA, D., GAMAL-ELDEEN, A. M., SALEH, S. & EL-DALY, S. M. 2014. The pharmacological effect of gum arabic on liver hyperplasia in the presence or absence of laser beam. Int J Innov Res Dev, 3, 269-73.

NEMMAR, A., AL-SALAM, S., BEEGAM, S., YUVARAJU, P. & ALI, B. H. 2019. Gum Arabic ameliorates impaired coagulation and cardiotoxicity induced by water-pipe smoke exposure in mice. Frontiers in physiology, 10, 53.

NG, K. W., KHOO, S. P., HENG, B. C., SETYAWATI, M. I., TAN, E. C., ZHAO, X., XIONG, S., FANG, W., LEONG, D. T. & LOO, J. S. 2011. The role of the tumor suppressor p53 pathway in the cellular DNA damage response to zinc oxide nanoparticles. Biomaterials, 32, 8218-8225.

PASUPULETI, S., ALAPATI, S., GANAPATHY, S., ANUMOLU, G., PULLY, N. R. & PRAKHYA, B. M. 2012. Toxicity of zinc oxide nanoparticles through oral route. Toxicology and industrial health, 28, 675-686.

RASMUSSEN, J. W., MARTINEZ, E., LOUKA, P. & WINGETT, D. G. 2010. Zinc oxide nanoparticles for selective destruction of tumor cells and potential for drug delivery applications. Expert opinion on drug delivery, 7, 1063-1077.

ROBERGE, S., ROUSSEL, J., ANDERSSON, D. C., MELI, A. C., VIDAL, B., BLANDEL, F., LANNER, J. T., LE GUENNEC, J.-Y., KATZ, A. & WESTERBLAD, H. 2014. TNF-α-mediated caspase-8 activation induces ROS production and TRPM2 activation in adult ventricular myocytes. Cardiovascular research, 103, 90-99.

ROY, R., PARASHAR, V., CHAUHAN, L., SHANKER, R., DAS, M., TRIPATHI, A. & DWIVEDI, P. D. 2014. Mechanism of uptake of ZnO nanoparticles and inflammatory responses in macrophages require PI3K mediated MAPKs signaling. Toxicology in Vitro, 28, 457-467.

SAVITSKAYA, M. & ONISHCHENKO, G. 2015. Mechanisms of apoptosis. Biochemistry (Moscow), 80, 1393-1405.

SENAPATI, V. A., KUMAR, A., GUPTA, G. S., PANDEY, A. K. & DHAWAN, A. 2015. ZnO nanoparticles induced inflammatory response and genotoxicity in human blood cells: A mechanistic approach. Food and Chemical Toxicology, 85, 61-70.

SHARMA, V., SINGH, S. K., ANDERSON, D., TOBIN, D. J. & DHAWAN, A. 2011. Zinc oxide nanoparticle induced genotoxicity in primary human epidermal keratinocytes. Journal of nanoscience and nanotechnology, 11, 3782-3788.

SUN, L., HUANG, Y., BIAN, Z., PETROSINO, J., FAN, Z., WANG, Y., PARK, K. H., YUE, T., SCHMIDT, M. & GALSTER, S. 2016. Sundew-inspired adhesive hydrogels combined with adipose-derived stem cells for wound healing. ACS applied materials & interfaces, 8, 2423-2434.

TANG, H.-Q., XU, M., RONG, Q., JIN, R.-W., LIU, Q.-J. & LI, Y.-L. 2016. The effect of ZnO nanoparticles on liver function in rats. International journal of nanomedicine, 4275-4285.

TANG, Y., XIN, H., YANG, S., GUO, M., MALKOSKE, T., YIN, D. & XIA, S. 2018. Environmental risks of ZnO nanoparticle exposure on Microcystis aeruginosa: Toxic effects and environmental feedback. Aquatic toxicology, 204, 19-26.

TESNIERE, A., PANARETAKIS, T., KEPP, O., APETOH, L., GHIRINGHELLI, F., ZITVOGEL, L. & KROEMER, G. 2008. Molecular characteristics of immunogenic cancer cell death. Cell Death & Differentiation, 15, 3-12.

TORABI, M., KESMATI, M., POURREZA, N., VARZI, H. N. & GALEHDARI, H. 2018. Neurobehavioral and biochemical modulation following administration of MgO and ZnO nanoparticles in the presence and absence of acute stress. Life sciences, 203, 72-82.

TURAN, B. & TUNCAY, E. 2017. Impact of labile zinc on heart function: from physiology to pathophysiology. International Journal of Molecular Sciences, 18, 2395.

VINARDELL, M. P. & MITJANS, M. 2015. Antitumor activities of metal oxide nanoparticles. Nanomaterials, 5, 1004-1021.

WANG, C., LU, J., ZHOU, L., LI, J., XU, J., LI, W., ZHANG, L., ZHONG, X. & WANG, T. 2016. Effects of long-term exposure to zinc oxide nanoparticles on development, zinc metabolism and biodistribution of minerals (Zn, Fe, Cu, Mn) in mice. PloS one, 11, e0164434.

WILLIAMS, P. A. & PHILLIPS, G. O. 2021. Gum arabic. Handbook of hydrocolloids. Elsevier.

WU, W., SAMET, J. M., PEDEN, D. B. & BROMBERG, P. A. 2010. Phosphorylation of p65 is required for zinc oxide nanoparticle–induced interleukin 8 expression in human bronchial epithelial cells. Environmental health perspectives, 118, 982-987.

YAN, Z., WANG, W., WU, Y., WANG, W., LI, B., LIANG, N. & WU, W. 2017. Zinc oxide nanoparticle-induced atherosclerotic alterations in vitro and in vivo. International Journal of Nanomedicine, 4433-4442.

YOUSEF, M. I., MUTAR, T. F. & KAMEL, M. A. E.-N. 2019. Hepato-renal toxicity of oral sub-chronic exposure to aluminum oxide and/or zinc oxide nanoparticles in rats. Toxicology reports, 6, 336-346.

YOUSEF, M. I., ROYCHOUDHURY, S., JAFAAR, K. S., SLAMA, P., KESARI, K. K. & KAMEL, M. A. E.-N. 2022. Aluminum oxide and zinc oxide induced nanotoxicity in rat brain, heart, and lung. Physiological research, 71, 677.

ZA'ABI, A., AL SALAM, S., AL SULEIMANI, Y., MANOJ, P., NEMMAR, A. & ALI, B. H. 2018. Gum acacia improves renal function and ameliorates systemic inflammation, oxidative and nitrosative stress in streptozotocin-induced diabetes in rats with adenine-induced chronic kidney disease. Cellular Physiology and Biochemistry, 45, 2293-2304.

ZAZUETA, C., BUELNA-CHONTAL, M., MACÍAS-LÓPEZ, A., ROMÁN-ANGUIANO, N. G., GONZÁLEZ-PACHECO, H., PAVÓN, N., SPRINGALL, R., ARANDA-FRAUSTO, A., BOJALIL, R. & SILVA-PALACIOS, A. 2018. Cytidine-5'-Diphosphocholine Protects the Liver From Ischemia/Reperfusion Injury Preserving Mitochondrial Function and Reducing Oxidative Stress. Liver Transplantation, 24, 1070-1083.

ZEID, I. M. A. & FARAJALLAH, A. R. 2018. Gum Arabic and Kidney Failure: An Exceptional Panacea. Gum Arabic. Elsevier.

ZERJATKE, T., GAK, I. A., KIROVA, D., FUHRMANN, M., DANIEL, K., GONCIARZ, M., MÜLLER, D., GLAUCHE, I. & MANSFELD, J. 2017. Quantitative cell cycle analysis based on an endogenous all-in-one reporter for cell tracking and classification. Cell reports, 19, 1953-1966.

ZHANG, M., DU, Y., LU, R., SHU, Y., ZHAO, W., LI, Z., ZHANG, Y., LIU, R., YANG, T. & LUO, S. 2016. Cholesterol retards senescence in bone marrow mesenchymal stem cells by modulating autophagy and ROS/p53/p21 Cip1/Waf1 pathway. Oxidative Medicine and Cellular Longevity, 2016.

ZHANG, Q., CHEN, K., WU, T. & SONG, H. 2019. Swertiamarin ameliorates carbon tetrachloride-induced hepatic apoptosis via blocking the PI3K/Akt pathway in rats. The Korean journal of physiology & pharmacology, 23, 21-28.

ZOHEIR, M., MEDWAR, A., SOLAIMAN, A. & ELBANAWANY, N. 2019. Histological Study of the Effect of Zinc Oxide Nanoparticles on the Cardiomyocytes of Adult Male Albino Rats with Reference to the Role of Mitochondria. Egyptian Journal of Histology, 42, 567-582.